RESEARCH ARTICLE

FBLIM1 Enhances Oral Cancer Malignancy via Modulation of the Epidermal Growth Factor Receptor Pathway†

Abbreviated title: FBLIM1 IN ORAL CANCER

Yuriko Toeda,[1] Atsushi Kasamatsu,[2*] Kazuyuki Koike,[1] Yosuke Endo-Sakamoto,[2] Kazuaki Fushimi,[3] Hiroki Kasama,[3] Yukio Yamano,[4] Masashi Shiiba,[5] Hideki Tanzawa,[1,2] Katsuhiro Uzawa[1,2*]

[1]Department of Oral Science, Graduate School of Medicine, Chiba University, Chiba, Japan
[2]Department of Dentistry and Oral-Maxillofacial Surgery, Chiba University Hospital, Chiba, Japan
[3]Department of Dentistry and Oral surgery, Eastern Chiba Medical Center, Chiba, Japan
[4]Department of Dentistry and Oral-Maxillofacial Surgery, Chibaken Saiseikai Narashino Hospital, Chiba, Japan
[5]Department of Medical Oncology, Graduate School of Medicine, Chiba University, Chiba, Japan

†This article has been accepted for publication and undergone full peer review but has not been through the copyediting, typesetting, pagination and proofreading process, which may lead to differences between this version and the Version of Record. Please cite this article as doi: [10.1002/mc.22889]

Additional Supporting Information may be found in the online version of this article.

Received 10 December 2017; Revised 28 July 2018; Accepted 15 August 2018
Molecular Carcinogenesis

DOI 10.1002/mc.22889

***Correspondence to**: Department of Dentistry and Oral-Maxillofacial Surgery, Chiba University Hospital, 1-8-1 Inohana, Chuo-ku, Chiba 260-8670, Japan

Tel: 81-43-226-2300, Fax: 81-43-226-2151

E-mail address: uzawak@faculty.chiba-u.jp

and

Department of Dentistry and Oral-Maxillofacial Surgery, Chiba University Hospital

1-8-1 Inohana, Chuo-ku, Chiba 260-8670, Japan

Tel: 81-43-226-2300, Fax: 81-43-226-2151

E-mail address: kasamatsua@faculty.chiba-u.jp

Grant support: The authors received no specific funding for this work. This research did not receive any specific grant from funding agencies in the public, commercial, or not-for-profit sectors.

Abbreviations: Akt, protein kinase B; DMEM, Dulbecco's modified Eagle medium; EGFR, epidermal growth factor receptor; EGM-2, endothelial growth medium-2; FBLIM1, filamin-binding LIM protein 1; GAPDH, glyceraldehyde-3-phosphate dehydrogenase; HNOKs, human normal oral keratinocytes; IHC, immunohistochemistry; JAK, Janus kinase; MAPK, mitogen-activated protein kinase; OSCC, oral squamous cell carcinoma; PI3K, phosphoinositide 3-kinase, qRT-PCR, quantitative reverse transcription-polymerase chain reaction; STAT, signal transducers and activator of transcription.

ABSTRACT

Filamin-binding LIM protein 1 (FBLIM1) is related to regulation of inflammatory responses, such as chronic recurrent multifocal osteomyelitis; however, the relevance of FBLIM1 in oral squamous cell carcinoma (OSCC) is unknown. The aim of the current study was to elucidate the possible role of FBLIM1 in the carcinogenesis of OSCC. We analyzed FBLIM1 expression using quantitative reverse transcriptase-polymerase chain reaction (qRT-PCR), immunoblot analysis, and immunohistochemistry. The expression levels of FBLIM1 were up-regulated significantly ($P < 0.05$) in OSCC-derived cell lines and primary OSCCs specimens compared with normal counterparts. FBLIM1 expression also was correlated with the primary tumoral size ($P < 0.05$) and vascular invasion ($P < 0.05$). We then assessed tumoral progression after treatment with FBLIM1 siRNA and clopidogrel, an antiplatelet agent. Similar to the FBLIM1 knockdown effect, clopidogrel-treated cells had attenuated functions of proliferation, migration, and invasiveness. Interestingly, clopidogrel treatment led to down-regulation of epidermal growth factor receptor (EGFR) and FBLIM1. These findings identify FBLIM1 as a putative therapeutic target by using clopidogrel for inhibiting over activation of EGFR signaling to prevent OSCC malignancy.

Keywords: clopidogrel, epidermal growth factor receptor, filamin-binding LIM protein 1, oral squamous cell carcinoma

This article is protected by copyright. All rights reserved

INTRODUCTION

Filamin binding LIM protein 1 (FBLIM1) was identified as a component of cell–extracellular matrix adhesions [1,2]. Filamins, cytoplasmic proteins that cross-link actin filaments, have been reported to coordinate the interaction between epidermal growth factor receptor (EGFR) and cytoskeleton [3-5].

FBLIM1 is related to inflammatory activity, including chronic recurrent multifocal osteomyelitis, and is found in several types of cancer, such as in the brain, liver, and breast [6-8]. Furthermore FBLIM1 is identified as an OSCC-related gene by our previous microarray data [9]. However, the relevance of FBLIM1 in oral squamous cell carcinoma (OSCC) is unknown.

The role of EGFR, a member of the transmembrane receptor tyrosine kinase family, has been studied extensively, which occurs the activation of the intracellular signaling pathway [10, 11]. EGFR regulates cellular processes, such as proliferation, survival, migration, and differentiation, and especially, EGFR internalization leads to restrained tumoral growth [12-14]. A clinical trial of anti-EGFR agents (i.e., cetuximab) for treating advanced OSCC emphasized the potential of EGFR as a target for anticancer therapy [15].

Clopidogrel, an antiplatelet agent that reduces the risks of myocardial infarction and stroke among high-risk patients [16], is associated with the EGFR pathway in rat gastric

epithelial cell [17]; however, the detailed mechanism in human derived cells is unclear.

In the current study, we sought to clarify the clinical relevance of FBLIM1 in OSCCs and evaluate a new candidate for medical treatment of OSCCs by drug repositioning of clopidogrel.

MATERIALS AND METHODS

Cells and Clinical Tissue Samples

OSCC-derived cell lines (HSC-2, HSC-3, HSC-4, KOSC-2, Sa3, Ca9-22, SAS, HO-1-u-1, and HO-1-N-1) were obtained from the Japanese Collection of Research Bioresources Cell Bank (Ibaraki, Osaka, Japan) or the RIKEN BioResource Center (Tsukuba, Ibaraki, Japan) [18,19]. All OSCC cell lines were cultured in Dulbecco's modified Eagle medium (DMEM) (Sigma-Aldrich, St. Louis, MO). We collected human normal oral keratinocytes (HNOKs), as normal controls in this research. Primary cultured HNOKs were grown in oral keratinocyte medium (ScienCell Research Laboratories, Carlsbad, CA). Human umbilical vein endothelial cells (Lonza Group Ltd., Basel, Switzerland) were propagated in Endothelial Growth Medium-2 (EGM-2) (Lonza Group Ltd.). All cells were cultured under standard conditions (37 ℃ and 5% CO_2).

This study was subject to approval by the ethics committee of Chiba University (protocol number, 236). HNOKs and one hundred one clinical OSCC specimens were obtained intraoperatively from three young non-tumoral patients and patients with OSCC, respectively after the patients provided informed consent for inclusion in this study at Chiba University Hospital. Respective normal tissue specimens also were obtained from each patient. Based on the World Health Organization criteria, histopathologic diagnoses of these specimens were performed at the Department of Pathology of Chiba University Hospital. The clinical stages of the OSCCs were determined according to the TNM classification [20].

mRNA Expression Analysis

We performed qRT-PCR as described previously [21-23]. The primer pairs and universal probes used were: *FBLIM1*: 5'-TTGAGAAAGGGGCATCCA-3' (forward); 5'-CCTCCACAGCCAGCTCTC-3' (reverse), probe #29; *GAPDH*: 5'-CATCTCTGCCCCCTCTGCTGA-3' (forward); and 5'-GGATGACCTTGCCCACAGCCT-3' (reverse), probe #60.

These primers were designed using the Universal Probe Library Assay Design Center (available at https://qpcr.probefinder.com/organism.jsp). qRT-PCR was conducted

to evaluate the expression levels of target mRNAs using the FastStart Essential DNA Probes Master (Roche Diagnostics, Mannheim, Germany) on the LightCycler 480 Instrument II (Roche Diagnostics). qRT-PCR reactions were performed in triplicate, and three independent preparations of RNA were analyzed from each cell line.

Immunoblot Analysis

Immunoblot analysis was conducted as described previously [24, 25]. The antibodies used were affinity-purified rabbit anti-FBLIM1 (1:1,000, HPA025287, Atlas Antibodies, Bromma, Sweden), EGFR (1:1000, #4267, Cell Signaling Technology, Danvers, MA), GAPDH (1:500, sc-32233, Santa Cruz, Dallas, TX), and horseradish peroxidase-conjugated anti-rabbit or anti-mouse IgG (H+L) (1:2,000, W401B and W4021, Promega, Madison, WI). Signals were developed by Clarity Western ECL Substrate (Bio-Rad, Hercules, CA) and visualization of protein bands was carried out by exposing the membranes to Bio-Rad ChemiDoc XRS system (Bio-Rad). The intensity of the signals was quantitated by Image Lab software (Bio-Rad). Densitometric FBLIM1 protein data were normalized to GAPDH protein levels.

Immunohistochemistry (IHC)

IHC was carried out as described previously [22, 26, 27]. The FBLIM1 IHC scores were calculated as the product of intensity multiplied by the percentage of positively staining cells. The intensity of the stained cells was classified into four levels, with 0+ indicating negative; 1+, low positive; 2+, positive; and 3+, high positive. FBLIM1 was classified as positive and negative using the median score of all tumors as the cut-off points [28]. Cases with a score over 118.03 were considered FBLIM1-positive.

Transfections

Two OSCC cells (HSC3, SAS) were transiently transfected with either FBLIM1 siRNA (sc-88837, Santa Cruz Biotechnology Inc.) or control siRNA (sc-37007, Santa Cruz Biotechnology Inc.) using Lipofectamine 3000 (Thermo Fisher Scientific, Waltham, MA) at a final concentration of 5 μM. To appraise the efficiency of FBLIM1 knockdown, we performed qRT-PCR and immunoblot analysis.

Proliferation Assay

For proliferation assessment, cells were seeded in 6-well plates at densities of $1.0x10^4$ viable cells/well. At the indicated time points, the cells were monitored using the trypan blue exclusion-based viable cell counting method [29].

Migration Assay

The cells were cultured in 6-well plates in medium with 10% fetal bovine serum (FBS) until a confluent monolayer formed tightly, after which one wound was created in the middle of each plate using a micropipette tip. The cells were washed, and the medium was replaced with serum-free medium. The results were visualized by measuring the wounded area at the indicated time points. To measure the wounded area, we used the Lenaraf220b free software (http://www.vector.co.jp/soft/dl/win95/art/se312811.html). The mean value was calculated from data obtained from six wells.

Invasion Assay

An invasion assay was performed as described previously [29]. Briefly, a total of $2.0x10^5$ cells in serum-free medium were plated in a Corning® BioCoat™ Matrigel® invasion chamber with 8.0 μm PET membranes in 6-well plates (Corning, Corning, NY). In the lower chamber, medium with 10% FBS was added as a chemoattractant. After 72 h, cells migrated through and attached to the bottom of the cell culture insert. The migrated cells were fixed with methanol and stained with crystal violet. To count the invading cells, images were captured randomly from five fields of vision at x100 magnification.

Transendothelial Migration

A transendothelial migration assay using the CytoSelect™ Tumor Transendothelial Migration Assay kit (Cell Biolabs, Inc., San Diego, CA) was performed according to the manufacturer's instructions. This assay was designed with an 8-μm pore size cell culture insert and a 24-well plate. Briefly, human umbilical vein endothelial cells were seeded into an upper chamber at a density of 1.0×10^5/well and placed on a well containing the endothelial cell growth medium prepared in advance. The cells were incubated for from 48 to 72 h until a monolayer formed tightly. Separately, a total of $1.0x10^6$ cells/ml of OSCC cells were suspended in a serum-free medium and labeled with a CytoTracker™ solution (Cell Biolabs, Inc.) for 1 h. Then, endothelial cell growth medium was removed and replaced by migration medium, and $3.0x10^5$ of the labeled cells were added on each upper chamber and further incubated for 24 h. Non-migrated cells in the upper chamber were removed with cotton swabs. The migratory cells were resolved in a cell lysis buffer and incubated 5 min at room temperature with shaking. The cell lysate was measured using the microplate reader TECAN Infinite 200 PRO (Tecan, M€annedorf, Switzerland) at 495 nm/520 nm (fluorescence).

Clopidogrel Treatment

Since clopidogrel (Selleck Chemicals, Houston, TX), an antiplatelet agent used to

prevent blood clots in peripheral vascular disease and cerebrovascular disease, is water-soluble at 25 °C or higher, clopidogrel was directly dissolved in the culture medium for further analyses. Cells were cultured with DMEM containing 10% FBS for 24 h and then challenged with 10 μM clopidogrel for 24 h at 37 °C. We used the clopidogrel-treated cells for functional analyses, such as cellular proliferation, migration, and invasiveness assays.

Immunofluorescence (IF)

For immunofluorescent staining, FBLIM1 knockdown and clopidogrel-treated cells were seeded on coverslips. At indicated time points, the cells were fixed with 4% paraformaldehyde and blocked with 0.5% bovine serum albumin. Subsequently, the cells were incubated with a primary anti-EGFR (#4267, Cell Signaling Technology) and incubated overnight at 4℃. The cells were washed with phosphate buffered saline and then incubated with the secondary antibody, goat anti-rabbit IgG (H+L) Alexa Fluor 488 (A-11008, Thermo Fisher Scientific) for 1 h at room temperature. Finally, the cells were counterstained with DAPI (ProLong™ Diamond Antifade Mountant with DAPI, Thermo Fisher Scientific). IF was observed using a confocal microscope, FV10i (Olympus Optical, Tokyo, Japan) and analyzed with the FluoView Software (Olympus Optical).

Statistical Analysis

Statistical differences were analyzed using the Student's t-test, $\chi 2$ test, Fisher's exact test, and Mann-Whitney U-test. $P < 0.05$ was considered statistically significant. The data are expressed as the mean ± standard error of the mean (SEM).

RESULTS

Up-Regulation of FBLIM1 in OSCC-Derived Cell Lines

To determine the biologic roles of *FBLIM1*, which was identified as a cancer-related gene by our previous microarray data [9], we first investigated the expression levels of FBLIM1 in nine OSCC-derived cell lines (HSC-2, HSC-3, HSC-4, KOSC-2, Sa3, Ca9-22, SAS, HO-1-u-1, and HO-1-N-1) and HNOKs using qRT-PCR and immunoblot analyses. *FBLIM1* mRNA was up-regulated significantly ($P < 0.05$) in all OSCC-derived cell lines compared with the HNOKs (Figure 1A). Figure 1B shows representative results of immunoblot analysis. The FBLIM1 protein expression increased in all OSCC-derived cell lines compared with the HNOKs.

Evaluation of FBLIM1 Expression in Primary OSCCs

Figure 1C and D, respectively, show representative IHC results for FBLIM1 protein in normal oral tissue and primary OSCCs. Strong FBLIM1 immunoreactivity was detected in the cytoplasm of OSCC tissues (Figure 1D), whereas the normal tissue showed almost negative immunostaining (Figure 1C). We analyzed the FBLIM1 protein expression in 101 primary OSCC specimens using the IHC scoring system [30]. The FBLIM1 IHC scores in normal oral tissues and OSCCs ranged from 0.3 to 164.1 (median, 53.1) and 26.2 to 223.2 (median, 118.3), respectively. The IHC scores in primary OSCCs were significantly ($P < 0.05$) higher than those in normal oral tissues (Figure 1E). Analysis of the correlation between FBLIM1 expression and clinical classifications indicated that FBLIM1 expression was correlated positively with T-primary tumor and vascular invasiveness ($P < 0.05$) (Table 1).

Establishment of FBLIM1 Knockdown Cells and Cellular Proliferation

To investigate the possibility of up-regulation of FBLIM1 as a cause of tumoral growth and vascular invasiveness in OSCCs, we depleted FBLIM1 protein from OSCC cells (HSC3 and SAS) by the siRNA technique. This resulted in down-regulation of FBLIM1 protein levels 48 h after transfection compared to cells transfected with control siRNA (Figure 2A).

To evaluate the effect of FBLIM1 knockdown on cellular growth, a proliferation assay was performed. The cellular growth of FBLIM1 siRNA transfected cells was inhibited markedly ($P < 0.05$) compared with control siRNA transfected cells after 72 h (Figure 2B).

FBLIM1 Promotes Cellular Migration, Invasiveness, and Transendothelial Migration

In the migration assay, the area wounded by a micropipette tip decreased significantly in FBLIM1 siRNA transfected cells after 12 h ($P < 0.05$). In contrast, the gap remained in FBLIM1 siRNA transfected cells after 12 h (Figure 3A). Analysis of invasiveness and transendothelial migration also showed lower invasiveness of OSCC cells treated with FBLIM1 siRNA compared with cells treated with control siRNA ($P < 0.05$) (Figure 3B, C). Taken together, these results agreed with our clinical data that showed that high FBLIM1 expression is associated with tumoral growth and vascular invasiveness (Table 1).

Clopidogrel Treatment

We challenged the cells with clopidogrel, an inhibitor of the EGFR pathway [17], for further analyses and found that FBLIM1 protein levels in the clopidogrel-treated cells

decreased obviously compared with the control cells (Figure 4A). The cellular growth of the clopidogrel-treated cells was inhibited significantly compared with the controls ($P < 0.05$) (Figure 4B). In the cellular migration assays, the clopidogrel-treated cells showed a gap after the 12-h treatment (Figure 5A). In addition, the number of clopidogrel-treated cells invading the pores decreased significantly ($P < 0.05$) after 72 h compared with the control cells (Figure 5B, C). These results indicated that clopidogrel induced down-regulation of FBLIM1 and might regulate critical functions associated with tumoral growth, migration, and invasiveness similar to the FBLIM1 siRNA transfected cells.

Clopidogrel Induces Down-Regulation and Internalization of EGFR

The cellular growth, migration, and invasiveness of OSCCs are linked biologically to activation of EGFR [31]. We measured the expression and localization of EGFR in FBLIM1 siRNA and clopidogrel-treated cells. In the former, the EGFR expression levels were suppressed markedly (Figure 6A). IF data showed that most of the EGFR was localized at the cellular membrane normally; however, FBLIM1 silencing caused internalization of EGFR in the FBLIM1 siRNA transfected cells (Figure 6B). Similar to the knockdown models, FBLIM1 and EGFR expression levels decreased significantly in clopidogrel-treated cells (Figure 6C), and internalization of EGFR was induced by

clopidogrel (Figure 6D). EGFR down-regulation by cetuximab revealed no contribution to down-regulation of FBLIM1 (Supplementary Figure 1). These results indicated that clopidogrel might lead to down-regulation and internalization of EGFR via FBLIM1.

DISCUSSION

The current results showed FBLIM1 overexpression in OSCC *in vitro* and *in vivo* and that FBLIM1 positivity in OSCC was correlated with tumoral growth and vascular invasion. FBLIM1 silencing was characterized by decreased cellular growth, invasiveness, and migratory activities (Figures 2, 3) and induced EGFR down-regulation. Surprisingly, clopidogrel, an antiplatelet drug, controlled FBLIM1 expression, leading to similar phenotypes of FBLIM1 knockdown cells.

In addition to a previous study that reported that FBLIM1 is up-regulated and promotes the migration of and invasive activities in human glioma cells [6], overexpression of FBLIM1 was found in OSCCs *in vitro* and *in vivo* (Figure 1). In contrast, FBLIM1 expression is down-regulated in breast cancer tissues and negatively correlated with regional lymph node metastasis in esophagus cancer [1, 8]. Thus, FBLIM1 plays pivotal roles in development and progression of several types of cancer.

Since FBLIM1 promotes migration and invasion in glioma cells through the EGFR

pathway [6], we investigated the cellular migratory and invasive activities in OSCCs and EGFR status using FBLIM1 knockdown experiments. EGFR internalization, which was challenged with ligands and various cellular stresses, caused down-regulation of EGFR by protein degradation [12-14]. IF data indicated that EGFR was trafficked from the cellular membrane to the cytoplasm, suggesting that FBLIM1 knockdown cells showed internalization of EGFR (Figure 6B). These results supported immunoblotting data (Figure 6A) that FBLIM1 knockdown induced down-regulation of EGFR.

Clopidogrel might contribute an antiplatelet effect and antitumoral activity [32]. Furthermore, clopidogrel is related closely related to the down-regulation of EGFR in rat gastric epithelial cells [17]; however, the detailed mechanism is unknown. Consistent with their study, our data showed that EGFR was internalized and down-regulated after clopidogrel treatment (Figure 6C, D). Interestingly, we found down-regulation of FBLIM1 in the clopidogrel-treated cells, indicating that FBLIM1 silencing and clopidogrel treatment took a similar pathway for down-regulation of EGFR. Suppression of EGFR reduces its downstream signals (PI3K/Akt, MAPK, and JAK/STAT3 pathways) associated with tumoral progression, such as tumoral growth and cellular invasiveness [10, 33]. Taken together, our data suggested strongly that the anticancer effect of clopidogrel led to down-regulation of EGFR via FBLIM1. This indicates the possibility that clopidogrel

might be a potential therapeutic agent with tumor-suppressing effect not only *in vitro* but also *in vivo*. Therefore, future studies are required to identify this possibility.

We concluded that FBLIM1, the upstream molecule of the EGFR pathway, is one of the key signals for OSCC progression and that clopidogrel might be a potential therapeutic agent with a certain tumor-suppressing effect in this disease.

ACKNOWLEDGEMENTS

We thank Ms. Lynda C. Charters for editing this manuscript. The authors received no financial support.

Competing Interests: The authors have no conflicts of interest to disclose.

REFERENCES

1. He H, Ding F, Li Y, *et al.* Migfilin regulates esophageal cancer cell motility through promoting GSK-3β-mediated degradation of β-catenin. *Mol Cancer Res*. 2012; 10: 273-81.

2. Gkretsi V, Zhang Y, Tu Y, *et al*. Physical and functional association of migfilin with cell-cell adhesions. *J Cell Sci.* 2005; 118:697-710.

3. Ylilauri M, Pentikäinen OT. MMGBSA as a tool to understand the binding affinities of filamin-peptide interactions. *J Chem Inf Model.* 2013; 53: 2626-33.

4. Ruskamo S, Gilbert R, Hofmann G, *et al*. The C-terminal rod 2 fragment of filamin A forms a compact structure that can be extended. *Biochem J.* 2012; 446: 261-9.

5. MacPherson M, Fagerholm SC. Filamin and filamin-binding proteins in integrin-regulation and adhesion. Focus on: "FilaminA is required for vimentin-mediated cell adhesion and spreading". *Am J Physiol Cell Physiol.* 2010; 298: C206-8.

6. Ou Y, Ma L, Dong L, *et al*. Migfilin protein promotes migration and invasion in human glioma through epidermal growth factor receptor-mediated phospholipase C-γ and STAT3 protein signaling pathways. *J Biol Chem*. 2012; 287: 32394-405.

7. Gkretsi V, Bogdanos DP. Experimental evidence of Migfilin as a new therapeutic target of hepatocellular carcinoma metastasis. *Exp Cell Res.* 2015; 334: 219-27.

8. Gkretsi V, Papanikolaou V, Zacharia LC, *et al*. Mitogen-inducible Gene-2 (MIG2) and migfilin expression is reduced in samples of human breast cancer. *Anticancer Res*. 2013; 3: 1977-81.

9. Yamano Y, Uzawa K, Shinozuka K, *et al*. Hyaluronan-mediated motility: A target in oral squamous cell carcinoma. *Int. J. Oncol.* 2008; 32: 1001-1009.

10. Yarden Y, Sliwkowski MX. Untangling the ErbB signalling network. *Nat Rev Mol Cell Biol.* 2001; 2: 127-37.

11. Sigismund S, Avanzato D, Lanzetti L. Emerging functions of the EGFR in cancer. *Mol Oncol.* 2018; 12: 3-20.

12. Waksal HW. Role of an anti-epidermal growth factor receptor in treating cancer *Cancer Metastasis Rev.* 1999; 18: 427-36.

13. Tomas A, Futter CE, Eden ER. EGF receptor trafficking: consequences for signaling and cancer. *Trends Cell Biol.* 2014; 24: 26-34.

14. Tan X, Lambert PF, Rapraeger AC, Anderson RA. Stress-Induced EGFR Trafficking: Mechanisms, Functions, and Therapeutic Implications. *Trends Cell Biol.* 2016; 26: 352-66.

15. Baselga J. The EGFR as a target for anticancer therapy--focus on cetuximab. *Eur J Cancer*. 2001; 37

16. Laura Dean, MD1 *Medical Genetics Summaries.* Created: March 8, 2012; Updated: November 19, 2015: 1-10.

17. Luo JC, Huo TI, Hou MC, *et al.* Clopidogrel delays gastric ulcer healing in rats. *Eur J Pharmacol.* 2012; 695: 112-9.

18. Tanzawa H, Uzawa K, Kasamatsu A, *et al*. Targeting gene therapies enhance sensitivity to chemo- and radiotherapy of human oral squamous cell carcinoma. *Oral sci int.* 2015; 12: 43-52.

19. Kasamatsu A, Uzawa K, Usukura K, *et al*. Loss of heterozygosity in oral cancer. *Oral sci int.* 2011; 8: 37-43.

20. Lh, G. Mk, C W. UICC TNM classification of Malignant tumors. 2009.

21. Koike K, Kasamatsu A, Iyoda M, *et al.* High prevalence of epigenetic inactivation of the human four and a half LIM domains 1 gene in human oral cancer. *Int. J. Oncol.* 2013;

42, 141-150.

22. Kimura Y, Kasamatsu A, Nakashima D, *et al.* ARNT2 Regulates Tumoral Growth in Oral Squamous Cell Carcinoma. *J. Cancer*. 2016; 7: 702-710.

23. Uzawa K, Kasamatsu A, Saito T, *et al.* Long-term culture of human odontoma-derived cells with a Rho kinase inhibitor. *Exp. Cell Res.* 2016; 347, 232-240.

24. Kasamatsu A, Uzawa K, Nakashima D, *et al.* Galectin-9 as a regulator of cellular adhesion in human oral squamous cell carcinoma cell lines. *Int. J. Mol. Med.* 2005; 16: 269-273.

25. Baba T, Sakamoto Y, Kasamatsu A, *et al.* Persephin: A potential key component in human oral cancer progression through the RET receptor tyrosine kinasemitogen-activated protein kinase signaling pathway. *Mol. Carcinog.* 2013; 617: 1-8.

26. Uzawa K, Ono K, Suzuki H, *et al.* High Prevalence of Decreased Expression of KAI1 Metastasis Suppressor in Human Oral Carcinogenesis. *Clin. Cancer. Res.* 2002; 8: 828-835.

27. Siiba M, Ishige S, Saito Y, *et al*. Down-regulated expression of family with sequence similarity 3, member B (FAM3B), in oral squamous cell carcinoma. *Oral sci int.* 2012; 9: 9-16.

28. Ronchetti L, Melucci E, De Nicola F, *et al*. DNA damage repair and survival outcomes in advanced gastric cancer patients treated with first-line chemotherapy. *Int J Cancer.* 2017; 140: 2587-2595.

29. Saito T, Kasamatsu A, Ogawara K, *et al.* Semaphorin7A promotion of tumoral growth and metastasis in human oral cancer by regulation of g1 cell cycle and matrix metalloproteases: Possible contribution to tumoral angiogenesis. *PLoS One.* 2015; 10: e0137923.

30. F. Varghese, A.B. Bukhari, R. Malhotra, A. De. IHC Profiler: an open source plugin for the quantitative evaluation and automated scoring of immunohistochemistry images of human tissue samples. *PloS One.* 2014; 9.

31. Vairaktaris E, Spyridonidou S, Goutzanis L, *et al*. Diabetes and oral oncogenesis. *Anticancer Res.* 2007; 27: 4185-93.

32. Leader A, Zelikson-Saporta R, Pereg D, *et al*. The Effect of Combined Aspirin and Clopidogrel Treatment on Cancer Incidence. *Am J Med.* 2017; 130: 826-832.

33. Zhen L, Fan D, Yi X, *et al*. Curcumin inhibits oral squamous cell carcinoma proliferation and invasion via EGFR signaling pathways. *Int J Clin Exp Pathol.* 2014; 7: 6438-46.

LEGENDS

Figure 1. Up-regulation of FBLIM1 expression in OSCC-derived cell lines and primary OSCCs. (A) The expression of *FBLIM1* mRNA is significantly (*$P < 0.05$, Student's t-test) increased in nine OSCC-derived cell lines compared with the HNOKs. Data are expressed as the mean ± SEM of triplicate experiments. (B) FBLIM1 protein expression is up-regulated in OSCC-derived cell lines compared with the HNOKs. (C, D) Representative FBLIM1 IHC staining of (C) normal tissue and (D) primary OSCC. Original magnification, x 400. In contrast to normal oral tissue, high immunoreactivity of FBLIM1 is seen in the OSCC tissue. (E) The FBLIM1 protein expression levels in OSCCs (n=101) are significantly (*$P < 0.05$, Student's t-test) higher than in normal oral tissues.

Figure 2. The effects of FBLIM1 knockdown cellular proliferation. (A) Down-regulation of FBLIM1 is detected 48 h after siRNA transfection by immunoblot analysis. (B) A cellular proliferation assay of FBLIM1 siRNA transfected OSCC cells. The cellular growth of FBLIM1 siRNA transfected cells is inhibited significantly (*$P < 0.05$) compared with the control siRNA transfected cells after 96 h. The results are expressed as the mean ± SEM of the values from three assays.

Figure 3. FBLIM1 promotes cellular migration, invasiveness, and transendothelial migration in FBLIM1 siRNA transfected cells. (A) Cellular migration assay. The wounded area is decreased significantly (*$P < 0.05$, Student's t-test) in the culture of control siRNA transfected cells after 12 h, whereas a gap remains in the FBLIM1 siRNA transfected cells. (B) Cellular invasion assay. Representative images of the invasive cells through Matrigel-coated membranes are shown. The number of FBLIM1 siRNA transfected cells penetrating through the micropores is decreased significantly (*$P < 0.05$, Student's t-test) compared with the control siRNA transfected cells. (C) Cellular transendothelial migration assay. The proportion of FBLIM1 siRNA transfected OSCCs migrating through an endothelial cell monolayer is decreased significantly (*$P < 0.05$, Student's t-test).

Figure 4. Clopidogrel treatment. (A) Immunoblot analysis of FBLIM1 protein levels in the clopidogrel-treated cells. The expression of FBLIM1 protein is lower in the clopidogrel-treated cells (clopidogrel concentration, 10 μM). (B) Proliferation assay of the clopidogrel-treated cells. The cellular growth of clopidogrel-treated cells (HSC3 and SAS) is inhibited compared with the control cells after 120 h. Clop, clopidogrel.

Figure 5. (A) Migration assay of the clopidgrel-treated cells. The wounded area is

decreased markedly (*$P < 0.05$, Student's t-test) in the culture of control cells after 12 h, whereas a gap remains in the clopidogrel-treated cells. (B) Invasiveness assay of the clopidogrel-treated cells. The number of clopidogrel-treated cells penetrating through the micropores is decreased significantly (*$P < 0.05$, Student's t-test) compared with the control cells. (C) Transendothelial migration of the clopidogrel-treated cells. The proportion of clopidogrel-treated cells migrating through an endothelial cell monolayer is decreased significantly (*$P < 0.05$, Student's t-test). Clop, clopidogrel.

Figure 6. Clopidogrel induces down-regulation and internalization of EGFR. (A) EGFR expression is analyzed by immunoblot analysis in FBLIM1 siRNA transfected cells. FBLIM1 siRNA transfected cells (HSC3 and SAS) show down-regulation of EGFR protein compared with control siRNA transfected cells. (B) The images of expression of EGFR in FBLIM1 siRNA transfected cells analyzed by IF. Most EGFR is localized at the cell membrane in control siRNA transfected cells. In contrast, FBLIM1 knockdown caused internalization of the EGFR. (C) The expression of EGFR in the clopidogrel-treated cells was analyzed by immunoblot analysis. The clopidogrel-treated cells (HSC3 and SAS) show down-regulation of FBLIM1 and EGFR compared with the control cells. (D) The images of expression of EGFR after treatment with clopidogrel for 48 h analyzed by IF. Most EGFR is localized at the cellular membrane; in contrast, treatment with

clopidogrel caused internalization of EGFR. Clop, clopidogrel.

Table 1. Correlation between FBLIM1 Expression and Clinical Classification in OSCCs

Clinical classification	Total	Results of Immunostaining No. of patients		*P* value
		FBLIM1-negative	FBLIM1-positive	
Age at surgery (years)				
<60	24	13	11	
≧60, <70	28	17	11	0.213[a]
≧70	49	20	29	
Gender				
Male	53	28	25	0.552[b]
Female	48	22	26	
T-primary tumor				
T1+T2	59	36	23	0.006[a*]
T3+T4	42	14	28	
N-regional lymph node				
Negative	67	33	34	1.00[b]
Positive	34	17	17	
Vascular invasiveness				
Negative	55	36	19	<0.001[b*]
Positive	46	14	32	
Stage				
I	22	14	8	
II	25	14	11	0.07[a]
III	13	8	5	
IV	41	14	27	
Histopathologic type				
Well	61	31	30	
Moderately	35	16	19	0.079[a]
Poorly	5	3	2	

*$P < 0.01$

[a]χ^2 test.

[b]Fisher's exact test.

Figure 1

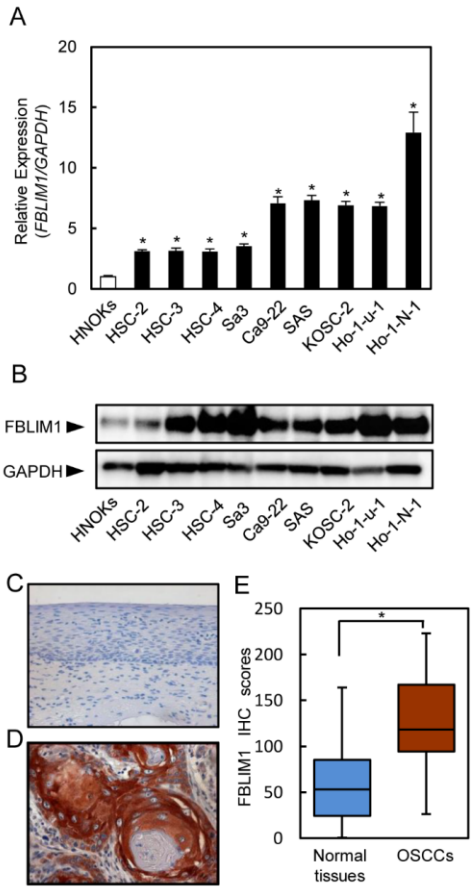

Figure 2

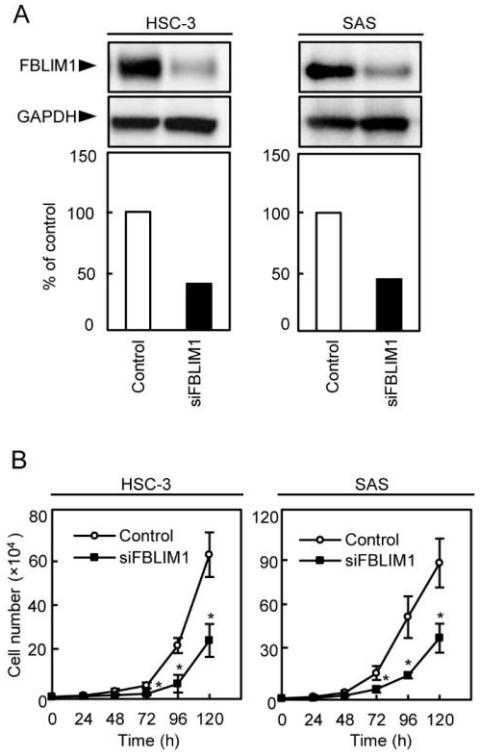

Figure 3

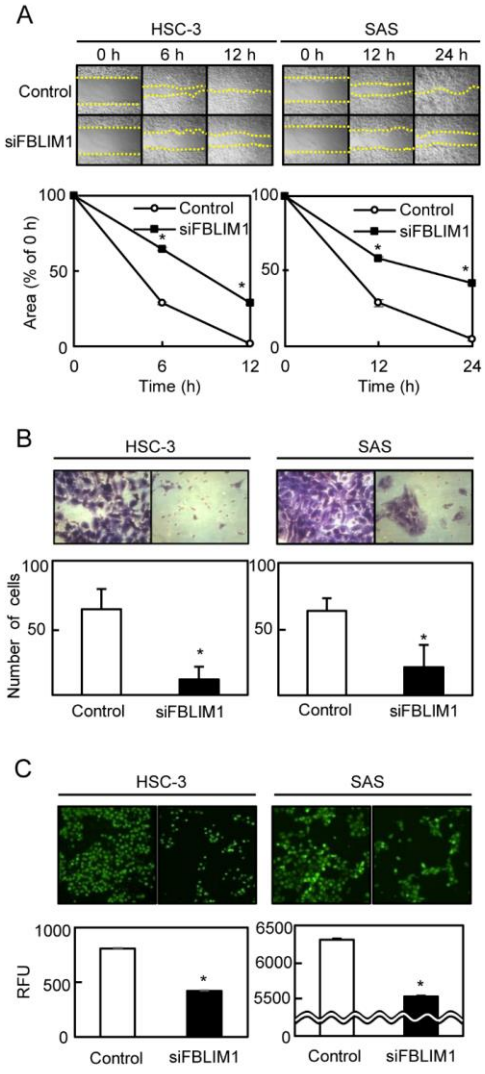

Figure 4

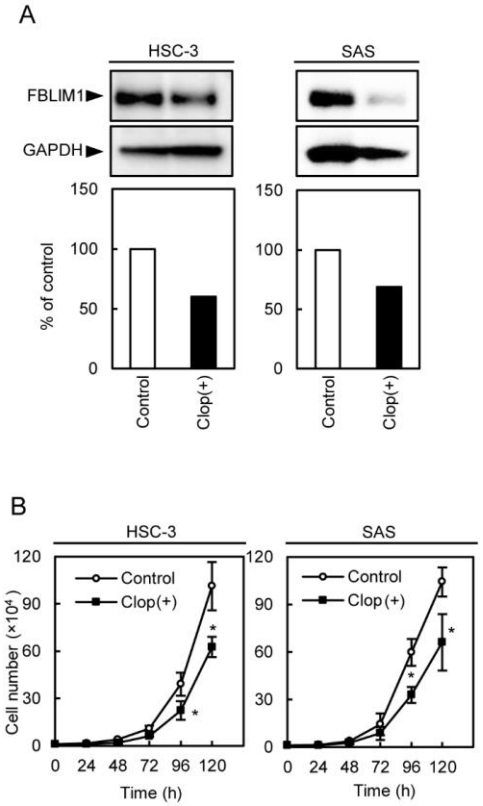

Figure 5

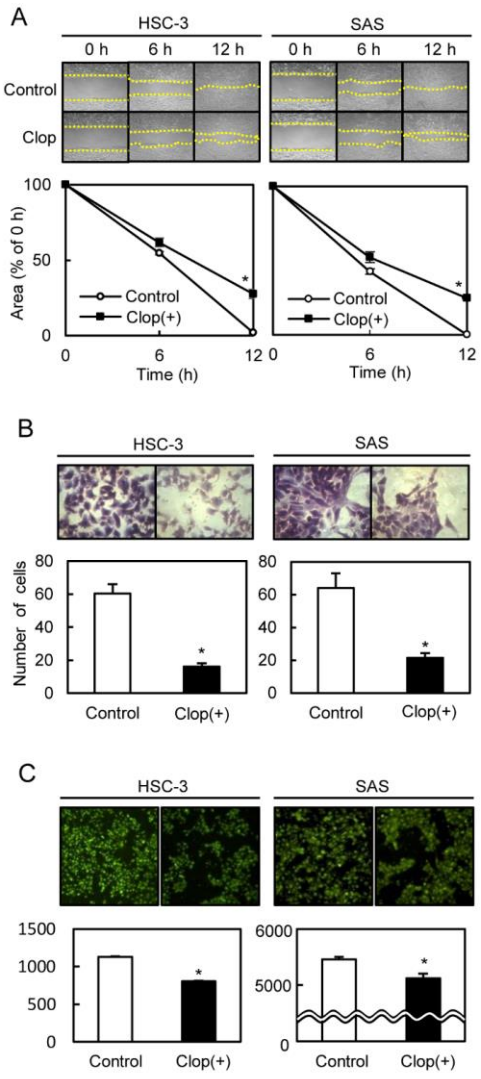

Figure 6